

Optical analog of Rabi oscillation suppression due to atomic motion

J. G. Muga* and B. Navarro†

Departamento de Química-Física, Universidad del País Vasco, Apdo. 644, 48080 Bilbao, Spain

(Received 13 May 2005; revised manuscript received 10 November 2005; published 22 February 2006)

The Rabi oscillations of a two-level atom illuminated by a laser on resonance with the atomic transition may be suppressed by the atomic motion through averaging or filtering mechanisms. The optical analogs of these velocity effects are described. The two atomic levels correspond in the optical analogy to orthogonal polarizations of light and the Rabi oscillations to polarization oscillations in a medium which is optically active, naturally or due to a magnetic field. In the latter case, the two orthogonal polarizations could be selected by choosing the orientation of the magnetic field, and one of them be filtered out. It is argued that the time-dependent optical polarization oscillations or their suppression are observable with current technology.

DOI: [10.1103/PhysRevA.73.022715](https://doi.org/10.1103/PhysRevA.73.022715)

PACS number(s): 32.80.-t, 42.25.Ja, 42.50.-p

I. INTRODUCTION

The analogies between phenomena occurring in two different physical systems open a route to find new effects or to translate solution techniques or devices, and quite often help to understand both systems better. The parallelism between light and atom optics, in particular, has been a strong driving force for fundamental and applied research, and it has received recently renewed impulse with the advent of laser cooling techniques, and Bose-Einstein condensation of alkali-metal gases. Atomic interferometers or atom lasers are important examples that illustrate the fruitfulness of this correspondence.

The analogy may also enable us to perform in one system experiments which are difficult to carry out in the other one. As an example, tunneling time experiments are much easier for microwaves than for matter waves [1,2], and the fact that the atoms are much slower than light, can be of great help in the analysis of time-dependent phenomena.

In this paper we shall describe the optical analogs of the time-dependent atomic Rabi oscillation in a laser field and of several dynamical suppression effects due to quantum, pure state atomic motion. The Rabi oscillation is at the heart of measurement procedures for time and frequency standards [3], photon number in a cavity [4], and other metrological applications [5,6], so its dynamic suppression may be a relevant effect, in particular for atomic clocks working with ultracold atoms. This suppression has been also proposed as a way to prepare specific internal atomic states by projection in quantum information applications [7].

The relation between light and atom optics is frequently established at the level of translational (external) degrees of freedom, but here we need, in addition, an optical parallel of the two internal levels of the atom, which is provided by the orthogonal states of light polarization. Thus we follow in reverse order, from matter to light, a connection that can be traced back historically to early experiments of Rabi, later modified by Ramsey, which lead to the development of

atomic clocks, and provided atomic analogs of polarization interferometry in optics, with the internal states of the atom or molecule playing the role of the polarization states of the photon [3,5,8].

For completeness a brief review of the dynamical suppression of the Rabi oscillation is provided in Sec. II, which is mostly based on Ref. [7] but incorporates also some new elements. Section III is devoted to the description of the optical analog. Section IV presents numerical illustrations. Section V describes a possible implementation of polarization filtering making use of magnetic fields.

II. RABI OSCILLATION SUPPRESSION FOR MOVING ATOMS

Neglecting decay, the effective Hamiltonian for a two level atom at rest and in presence of a detuned laser field is

$$H = \frac{\hbar}{2} \begin{pmatrix} 0 & \Omega \\ \Omega^* & -2\delta \end{pmatrix}, \quad (1)$$

where Ω is the on-resonance Rabi frequency, $\delta = \omega_L - \omega$ is the detuning (ω_L being the laser frequency and ω the atomic frequency) and internal ground and excited states are represented as $|1\rangle \equiv \begin{pmatrix} 1 \\ 0 \end{pmatrix}$ and $|2\rangle \equiv \begin{pmatrix} 0 \\ 1 \end{pmatrix}$, respectively. If at time zero the atom is in the ground state, the ground and excited components of the state evolved with this Hamiltonian are

$$\psi^{(1)} = e^{i\delta t/2} [\cos(\Omega' t/2) - (i\delta/\Omega') \sin(\Omega' t/2)], \quad (2)$$

$$\psi^{(2)} = e^{i\delta t/2} [(-i\Omega/\Omega') \sin(\Omega' t/2)], \quad (3)$$

so that the populations $|\psi^{(1,2)}|^2$ alternate oscillating harmonically in time with “Rabi period” $2\pi/\Omega'$ and effective Rabi frequency $\Omega' \equiv (\delta^2 + |\Omega|^2)^{1/2}$. The oscillation may, however, be suppressed when the atoms move into a region illuminated by a perpendicular laser beam [7]. For an idealized sharp laser profile in a one-dimensional approximation (its validity and the three-dimensional case are examined in Ref. [9]), the Hamiltonian becomes

*Email address: jg.muga@ehu.es

†Email address: qfbnatob@lg.ehu.es

$$H = \hat{p}^2/2m + \frac{\hbar}{2}\Theta(\hat{z})\begin{pmatrix} 0 & \Omega \\ \Omega^* & -2\delta \end{pmatrix}, \quad (4)$$

where \hat{z} and \hat{p} are position and momentum operators, and Θ is the Heaviside function. If reflection is negligible, for moderate to high velocities, the stationary eigenfunction for incidence in the ground state with wave number k can be approximated, up to a normalization constant, as

$$\begin{aligned} \phi_k^{(1)} &\approx e^{ikz} e^{i\delta t/2} \left[\cos\left(\frac{\Omega'zm}{2\hbar k}\right) - (i\delta/\Omega') \sin\left(\frac{\Omega'zm}{2\hbar k}\right) \right], \\ \phi_k^{(2)} &\approx e^{ikz} e^{i\delta t/2} \left[(-i\delta/\Omega') \sin\left(\frac{\Omega'zm}{2\hbar k}\right) \right]. \end{aligned} \quad (5)$$

Comparing with Eqs. (2) and (3), this expression reveals a spatial Rabi oscillation where the quantity $zm/\hbar k$ plays the role of time in the arguments of the trigonometric functions. Note also the additional plane wave factor with momentum $k\hbar$ denoting the translation of the center of mass. In other words, the Rabi oscillation is also evident spatially in the stationary eigenstates, under the form of density undulations of the two components with a ‘‘Rabi wavelength’’ $\lambda_R = \hbar/m\Omega'$.

The Rabi oscillation may be suppressed ‘‘adiabatically’’ if a quasimonochromatic, pure-state wave packet enters slowly into the laser illuminated region. In the quasimonochromatic regime the time dependent wave function may be approximately factorized into translational and internal factors as in Eq. (5), with the translational factor describing the spatial location of the packet for a given time. If this localization is sharp with respect to λ_R , the z in the internal factor may be substituted by a classical, well defined position, $z(0) + (k\hbar/m)t$, so that the z -integrated populations oscillate once the packet has entered the laser region at $z=0$, for $t_{\text{ent}} = -z(0)m/(k\hbar)$. However, if the wave packet is broad with respect to λ_R , or equivalently, the time interval required by the packet to enter into the laser region is greater than the Rabi period, the average over z to get the populations cancels the oscillation out. Note that this oscillation suppression in the quasi-monochromatic regime is not due to an average over different frequencies but to a phase averaging. Intuitively, and according to a classical picture, the atoms in the ensemble start to oscillate at different times because of their different entrance instants corresponding to a significant spread of the initial values $z(0)$. This intuitive interpretation cannot be taken too literally though. In particular, the suppression involves a pure state and not a statistical mixture. Note also that no incoherent ‘‘fading’’ due to decay from the excited state is involved. (The effect of fading was discussed in Ref. [7].)

A second group of suppression effects is associated with state filtering or velocity splitting. To explain these two related concepts, we need a more accurate representation than before. In the laser region, let $|\lambda_+\rangle$ and $|\lambda_-\rangle$ be the eigenstates, corresponding to the eigenvalues λ_\pm , of the matrix $\frac{1}{2}\begin{pmatrix} 0 & \Omega \\ \Omega^* & -2\delta \end{pmatrix}$. One easily finds

$$\lambda_\pm = \frac{-\delta \pm \Omega'}{2}, \quad (6)$$

$$|\lambda_\pm\rangle = \begin{pmatrix} 1 \\ -\frac{\delta \pm \Omega'}{\Omega} \end{pmatrix}, \quad (7)$$

where $|\lambda_\pm\rangle$ have not been normalized. [For later comparison with ‘‘circularly polarized states’’ notice that by setting $\delta=0$ and for the case $\Omega=i|\Omega|$, $\lambda_\pm = \pm\Omega/2$, and $|\lambda_\pm\rangle = \begin{pmatrix} 1 \\ \mp i \end{pmatrix}$.] The stationary state for $z>0$ can be written as a superposition

$$\Phi_k(z) = C_+|\lambda_+\rangle e^{ik_+z} + C_-|\lambda_-\rangle e^{ik_-z}, \quad (8)$$

where

$$k_\pm = k \left(1 - \frac{m(-\delta \pm \Omega')}{\hbar k^2} \right)^{1/2}, \quad (9)$$

and the coefficients C_\pm are obtained from the matching conditions at $z=0$ [7]. The two components (\pm) have two different propagation velocities and in fact the Rabi oscillation may be understood as an interference between the two terms when $k_\pm \approx k + m(\delta \mp \Omega')/(2\hbar k)$. For initially quasimonochromatic packets, with the wave number spread much smaller than the average wave number $\sigma_k/k_0 \ll 1$, the two different velocities also imply eventually a spatial separation of the $|\lambda_\pm\rangle$ components, so that the interference and associated Rabi oscillation finally disappear for times larger than the time to split the packet into two, $2\sigma_z k/\Omega'$, where σ_z^2 is the spatial variance of the wave packet. An extreme case is the complete state filtering that occurs for very low kinetic energies, when k_- is purely imaginary so that e^{ik_-z} becomes an evanescent wave and only the $|\lambda_+\rangle$ component survives in the laser region for z greater than the penetration length $[\text{Im}(k_-)]^{-1}$. Since the exact form of the surviving $|\lambda_+\rangle$ state can be modified by the laser detuning and Rabi frequency, this state filtering effect provides a projection mechanism to prepare specific internal states regardless of the incident atomic state [7].

III. OPTICAL ANALOG

In the optical analog of the dynamic effects described, the internal states will be substituted by orthogonal polarizations of the field, and the laser region by an optically active medium; the rotation of the polarization plane and corresponding oscillation of the linear polarization intensities will mimic the Rabi oscillation, and electromagnetic pulses will play the role of the atomic wave packets.¹

The use of a complex electric field for quasimonochromatic pulses within analytic signal theory facili-

¹One further correspondence may be established with a spin-polarized electron incident on a region with a perpendicular magnetic field, i.e., there is an analogy between Rabi oscillations and Larmor precession, which has been used to extend the concept of a Larmor clock [10,11] and other definitions of a traversal time to atomic systems [11–18].

tates the comparison and correspondence between quantum wave function and electric field components. Some of the parallelisms are quite direct. For example, we shall keep the same notation for the quantum wave numbers and the optical propagation constants k and k_{\pm} , or for the coefficients in the stationary waves, such as C_{\pm} and the reflection amplitudes R , although their values and detailed expressions need not be equal. Atomic populations in the ground state may be related to total energies in the vertical, linear polarization component and, similarly, the atomic excited state will be mimicked by horizontal, linear polarization. In our analogy, positions and times are present both in optics and quantum mechanics since we want to describe and compare pulses and wave packets in space-time. This is at variance with the analogy established by Zaspaskii and Kozlov [19], in which the spatial coordinate played the role of time in a Schrödinger-like equation satisfied by the polarization vector. From the Maxwell equations in a nonmagnetic, electrically neutral dielectric medium, the wave equation for the \mathbf{E} field of a harmonic, plane wave solution is

$$\mathbf{k}_m \times (\mathbf{k}_m \times \mathbf{E}) + \frac{\omega^2}{c^2} \mathbf{E} = -\frac{\omega^2}{c^2} \boldsymbol{\chi} \mathbf{E}, \quad (10)$$

where the subscript m in k_m stands for “medium” and it will be used to avoid confusion with $k = \omega/c$ in vacuum. $\boldsymbol{\chi}$ is the susceptibility tensor,

$$\boldsymbol{\chi} = \begin{bmatrix} \chi_{11} & \chi_{12} & \chi_{13} \\ \chi_{12}^* & \chi_{22} & \chi_{23} \\ \chi_{13} & \chi_{23} & \chi_{33} \end{bmatrix}. \quad (11)$$

The medium is assumed to be nonabsorbing so that $\boldsymbol{\chi}$ is Hermitian. The absorbing case is briefly considered in Sec. V and in the Appendix.

Written in components, Eq. (10) leads to

$$E_z = -(\chi_{13}^* E_x + \chi_{23}^* E_y) / \gamma_3 \quad (12)$$

and the system

$$\begin{aligned} \left[-k_m^2 + \frac{\omega^2}{c^2} \left(\gamma_1 - \frac{|\chi_{13}|^2}{\gamma_3} \right) \right] E_x + \frac{\omega^2}{c^2} \left(\chi_{12} - \frac{\chi_{13} \chi_{23}^*}{\gamma_3} \right) E_y &= 0, \\ \frac{\omega^2}{c^2} \left(\chi_{12}^* - \frac{\chi_{23} \chi_{13}^*}{\gamma_3} \right) E_x + \left[-k_m^2 + \frac{\omega^2}{c^2} \left(\gamma_2 - \frac{|\chi_{23}|^2}{\gamma_3} \right) \right] E_y &= 0, \end{aligned} \quad (13)$$

where $\gamma_j \equiv 1 + \chi_{jj}$. It can be solved by making the determinant of the coefficients vanish, and the result is a fourth order equation ($k_m^4 + \alpha k_m^2 + \beta = 0$).

Since we shall assume that the wave incides from a vacuum region adjacent to a semi-infinite medium, we only pick up two physical solutions (if complex they must have a positive imaginary part to decay; if real they must be positive to implement outgoing boundary conditions) and denote them as k_{\pm} ,

$$k_{\pm} = \frac{\omega}{c} n_{\pm}, \quad (14)$$

n_{\pm} being the corresponding refraction index. Examples will be given soon.

The polarization corresponding to each solution in the x - y plane, up to an intensity constant, may be given in terms of the Jones vector $\begin{bmatrix} E_x \\ E_y \end{bmatrix}_{\pm}$ [20]. For a closer comparison with the atomic case we may use the notation $E^{(1)} \equiv E_x$, $E^{(2)} \equiv E_y$, reminiscent of the atomic ground- and excited-state amplitudes. In particular, the internal atomic states $\begin{pmatrix} 1 \\ 0 \end{pmatrix}$ (ground) and $\begin{pmatrix} 0 \\ 1 \end{pmatrix}$ (excited) correspond to the Jones vectors $\begin{bmatrix} 1 \\ 0 \end{bmatrix}$, $\begin{bmatrix} 0 \\ 1 \end{bmatrix}$ which denote, respectively, “vertical” (x direction) and “horizontal” (y direction) linear polarization.

Since we are not specifying the total intensity, the polarization is also represented by any proportional vector. In particular, it is convenient to work with

$$|\lambda_{\pm}\rangle = \begin{bmatrix} 1 \\ \left(\frac{E_y}{E_x} \right)_{\pm} \end{bmatrix}, \quad (15)$$

where

$$\left(\frac{E_y}{E_x} \right)_{\pm} = \frac{\gamma_1 - \frac{|\chi_{13}|^2}{\gamma_3} - \frac{k_{\pm}^2 c^2}{\omega^2}}{-\chi_{12} + \chi_{13} \chi_{23}^* / \gamma_3}. \quad (16)$$

Depending on the value of $(E_y/E_x)_{\pm} = a + ib$ (a and b real), the polarization can be linear ($b=0$), circular ($a=0, b=\pm 1$), or in general elliptic.

For an optically active medium with a susceptibility tensor of the form

$$\boldsymbol{\chi} = \begin{bmatrix} \chi_{11} & \chi_{12} & 0 \\ \chi_{12}^* & \chi_{11} & 0 \\ 0 & 0 & \chi_{33} \end{bmatrix}, \quad \text{Re}(\chi_{12}) = 0, \quad (17)$$

the optical propagation constants are given by

$$k_{\pm} = \frac{\omega}{c} (1 + \chi_{11} \pm |\chi_{12}|)^{1/2}. \quad (18)$$

Assuming $\text{Im}(\chi_{12}) > 0$, two orthogonal harmonic solutions for right (+) and left (−) circularly polarized light, forward-moving or possibly evanescent (if k_{-} becomes imaginary) are

$$\begin{bmatrix} 1 \\ -i \end{bmatrix} e^{ik_+ z} e^{-i\omega t}, \quad \begin{bmatrix} 1 \\ i \end{bmatrix} e^{ik_- z} e^{-i\omega t}, \quad (19)$$

In vacuum, we have instead $\boldsymbol{\chi} = \mathbf{0}$, and the following forward/backward moving orthogonal harmonic solutions (with signs $+/-$, respectively)

$$\begin{bmatrix} 1 \\ 0 \end{bmatrix} e^{\pm ikz} e^{-i\omega t}, \quad \begin{bmatrix} 0 \\ 1 \end{bmatrix} e^{\pm ikz} e^{-i\omega t}, \quad (20)$$

where $k = \omega/c > 0$.

If the optically active medium occupies the region $z > 0$, and for normal incidence (\mathbf{k} in z direction) of vertically polarized light, the harmonic solution reads, up to a constant $e^{-i\omega t} \mathbf{F}_k(z)$, where

$$\mathbf{F}_k(z) = \begin{cases} \begin{bmatrix} 1 \\ 0 \end{bmatrix} (e^{ikz} + R_{11}e^{-ikz}) + \begin{bmatrix} 0 \\ 1 \end{bmatrix} R_{21}e^{-ikz}, & z < 0, \\ C_+ \begin{bmatrix} 1 \\ -i \end{bmatrix} e^{ik_+z} + C_- \begin{bmatrix} 1 \\ i \end{bmatrix} e^{ik_-z}, & z > 0. \end{cases} \quad (21)$$

Imposing at $z=0$ the continuity of the tangential components of the electric and magnetic fields amounts, for normal incidence, to enforce the continuity of the components $E_{x,y}$ and their derivatives. Solving the resulting system,

$$R_{11} = \frac{k_+k_- - k^2}{(k+k_+)(k+k_-)}, \quad C_+ = \frac{k}{k+k_+}, \quad (22)$$

$$R_{21} = \frac{-ik(k_- - k_+)}{(k+k_+)(k+k_-)}, \quad C_- = \frac{k}{k+k_-}. \quad (23)$$

There are thus two propagation constants k_{\pm} , and two group velocities in the optically active medium

$$\frac{d\omega}{dk_{\pm}} = \frac{c}{n_{\pm}}. \quad (24)$$

When $|\chi_{11}|, |\chi_{12}| \ll 1$, the two propagation constants differ only slightly,

$$k_{\pm} \approx \frac{\omega}{c} \left(1 + \frac{\chi_{11} \pm |\chi_{12}|}{2} \right), \quad (25)$$

there is also negligible reflection $R_{j1} \approx 0$ ($j=1,2$) and $C_{\pm} \approx 1/2$, so that in the optically active medium $z > 0$,

$$E^{(1)} \approx e^{i(kz-\omega t)} \cos(k|\chi_{12}|z/2), \quad (26)$$

$$E^{(2)} \approx e^{i(kz-\omega t)} \sin(k|\chi_{12}|z/2). \quad (27)$$

Each z is thus characterized by some linear polarization that rotates when z increases (optical activity). The rotation length for a full cycle of the moduli squared is $L = 2\pi c/\omega|\chi_{12}|$ or, equivalently, the cycle requires a time $T = 2\pi/\omega|\chi_{12}|$ for a quasimonochromatic pulse. Pulses are analogous to wave packets in the present correspondence and are formed by superposition of harmonic components. Moreover, in the quasi-monochromatic regime, we can interpret the modulus squared of complex field components as (half) short time averages of the real field, according to the theory of complex analytic signals [21]. Up to a constant that fixes the actual intensity, the time dependent field is given by

$$\mathbf{E}(z,t) = \frac{1}{(2\pi)^{1/2}} \int_0^{\infty} dk A(k) \mathbf{F}_k(z) e^{-i\omega t}. \quad (28)$$

The time δ_t required, from the entrance instant of the pulse peak, to split the pulse into two separated pulses of orthogonal circular polarization may be estimated by imposing that the spatial increment between the two components, due to

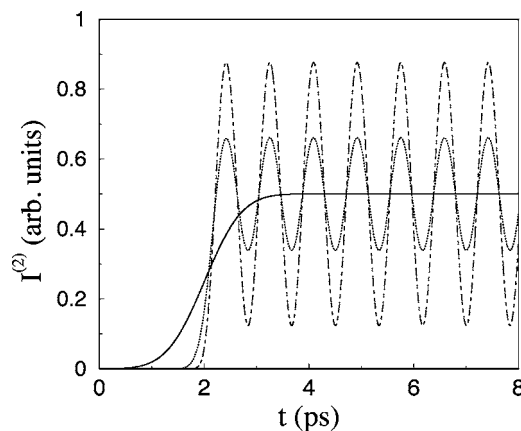


FIG. 1. Oscillation suppression due to slow (adiabatic) entrance in the optically active medium. $I^{(2)}(t)$ is represented for different pulse widths: $\sigma_t=100$ fs (dotted-dashed line); $\sigma_t=200$ fs (dotted line); $\sigma_t=600$ fs (solid line). $\chi_{11}=0$, $\chi_{12}=0.002$. The pulse is given in Eqs. (28) and (31) with $z_0=-600 \mu\text{m}$ and $\lambda_0=500$ nm.

their different group velocities, be equal to the pulse width σ_z . In particular, for $\chi_{11}=0$ and $|\chi_{12}| \ll 1$,

$$\delta_t = \frac{2\sigma_t}{|\chi_{12}|}, \quad (29)$$

where $\sigma_z = \sigma_t/c$. A time dependent observation of the polarization rotation, which is the optical analog of a temporal Rabi oscillation, requires $\delta_t > T$ to avoid the splitting, but also $\sigma_t < T$ to avoid an averaging suppression. Combining the two constraints gives the ideal conditions

$$\chi_{12} \ll \frac{\sigma_k}{k_0} \ll 1. \quad (30)$$

IV. NUMERICAL EXAMPLE

In this section we shall demonstrate with numerical examples the time dependence of the polarization rotation in the optically active medium and several dynamical suppression effects. The pulse is chosen within the quasimonochromatic regime, so that we may neglect any variation with k of the matrix elements of the susceptibility and consider constant values in each calculation. We have used Eq. (28) with the Gaussian amplitude

$$A(k) = \sqrt{\sigma_z} \left(\frac{2}{\pi} \right)^{1/4} e^{-(k-k_0)^2 \sigma_z^2} e^{-ikz_0}. \quad (31)$$

It is for convenience “normalized” so that $\int dk |A(k)|^2 = 1$ and, at time zero, $\int dz |E^{(1)}(z, t=0)|^2 = 1$. In all cases the central wavelength is chosen in the visible region of the spectrum, $\lambda_0 = 2\pi/k_0 = 500$ nm. The pulse is thus a right moving Gaussian pulse of vertically polarized light centered at time $t=0$ at $z_0 < 0$, outside the optically active medium, and with spatial variance σ_z^2 .

Figure 1 shows the oscillation of the integrated polarization intensity $I^{(2)}$,

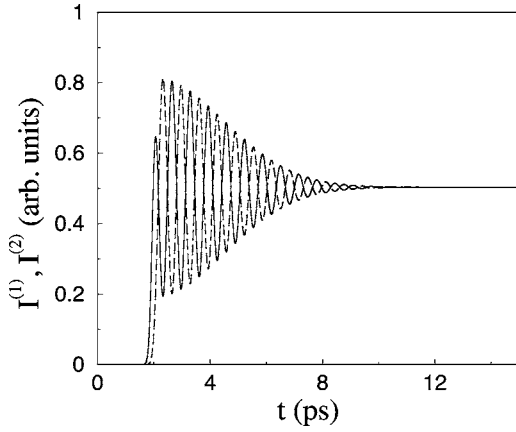


FIG. 2. Oscillation suppression of the integrated polarization intensities due to pulse splitting: $I^{(1)}$ (solid line) and $I^{(2)}$ (dashed line). $\chi_{12}=0.08$, $\sigma_r=100$ fs, and other parameters as in Fig. 1. A transition time that separates the two regimes (with or without rotation) may be estimated as the time for the arrival of the pulse peak at the medium plus the splitting time of Eq. (29). This gives 4.5 ps for the present parameters.

$$I^{(j)}(t) \equiv \int_0^\infty dz |E^{(j)}(z,t)|^2, \quad j=1,2, \quad (32)$$

proportional to the total energy in horizontal linear polarization within the optically active medium versus time. Whereas optical activity is standardly considered in coordinate space and measured in stationary conditions at the end of a slab, here we adopt a different, time dependent view, closer to the quantum Rabi oscillation analog.

If the pulse duration is much smaller than the rotation period, the oscillation is clearly visible. If the pulse width is increased and becomes comparable or larger than the rotation wavelength, however, the oscillation is suppressed. This is the optical analog of the adiabatic suppression of the Rabi oscillation due to a slow entrance of the atoms in the laser region.

An interesting phenomenon occurs if the observation time is large enough so that the pulse splits as a consequence of the two different group velocities. This is shown in Fig. 2, where the oscillation eventually fades away because of the progressive lack of interference between the two circularly polarized components.

Finally, the rotation suppression by filtering, analogous to atomic state filtering, is illustrated in Fig. 3. The left circular polarization becomes evanescent for the chosen susceptibility $\chi_{11}=0$ and $\chi_{12}=1.2$, so, after a transient, the pulse in the active medium is only composed by right handed circular polarization, see Fig. 3(b), where the total intensities

$$I^\pm = \int_0^\infty dz |E^{(\pm)}|^2 \quad (33)$$

are represented versus time. The absence of left-handed polarization after the transient peak precludes any oscillation of the linear polarization intensities $I^{(1,2)}$, as shown in Fig. 3(a).

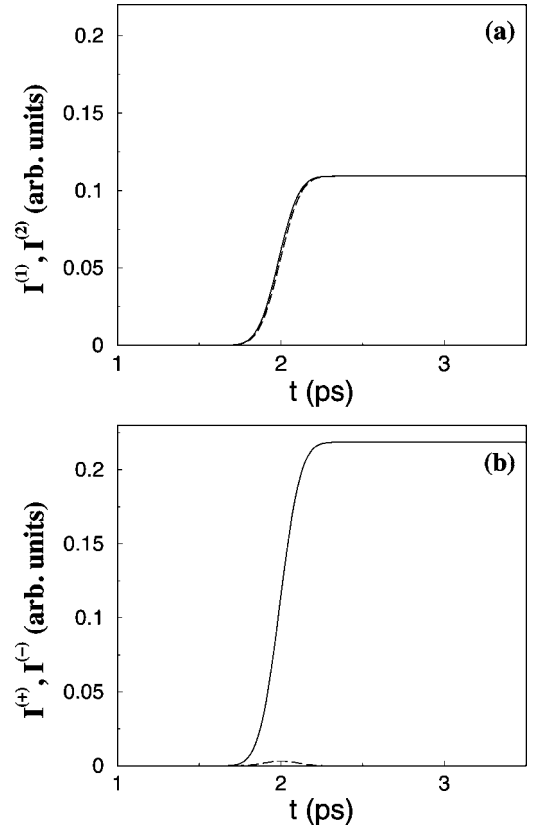


FIG. 3. Oscillation suppression of the integrated polarization intensities due to filtering. $\chi_{12}=1.2$, $\sigma_r=100$ fs, and other parameters as in Fig. 1. In (a) we show the vertical (solid line) and horizontal (dashed line) polarization components and in (b) the right (solid line) and left (dashed line) circular polarization components.

V. MAGNETO-OPTIC EFFECTS

Instead of finding materials with the susceptibility tensors necessary to observe the different suppression effects, it is possible to manipulate χ for an isotropic dielectric by applying a static magnetic field \mathbf{B} . The susceptibility tensor elements in terms of the resonance frequency ω_0 , plasma frequency ω_p , and cyclotron frequencies ω_{cu} , $u=x,y,z$, is given in the Appendix for a simple Lorentz model. Let us first examine the ‘‘Faraday configuration,’’ with the magnetic field along the z direction. In that case the susceptibility takes the form given in Eq. (17) and the solutions k_\pm correspond to two orthogonal circular polarizations.

If instead the selected magnetic field direction is x (Cotton-Mouton configuration), the form of the susceptibility tensor becomes

$$\chi = \begin{bmatrix} \chi_{11} & 0 & 0 \\ 0 & \chi_{33} & \chi_{23} \\ 0 & \chi_{23}^* & \chi_{33} \end{bmatrix}, \quad \text{Re}(\chi_{23}) = 0, \quad (34)$$

which leads to modes with linear polarizations in x and y directions. A field \mathbf{B} in an arbitrary direction between the Faraday and the Cotton-Mouton configurations produces, in general, two elliptic polarizations.

Let us determine the conditions which make one, and only one, of the propagation constants evanescent, to achieve polarization state filtering and selection. We shall work out in detail the Faraday configuration, but the Cotton-Mouton case or some other magnetic field orientation could be treated similarly. For the Faraday configuration, k_{\pm} are either purely real or purely imaginary, and the parameter regions in which one wave becomes evanescent are delimited by the zeros of k_{\pm} , which correspond, respectively, to

$$1 + \chi_{11} = \mp |\chi_{12}|, \quad (35)$$

see Eq. (18). Using the expressions for χ_{11} and χ_{12} given in the Appendix, Eq. (35) becomes

$$1 + \frac{\omega_p^2}{[(\omega_0^2 - \omega^2)^2 - \omega^2 \omega_{cz}^2]} = \pm \left| \frac{\omega_p^2 \omega \omega_{cz}}{[(\omega_0^2 - \omega^2)^2 - \omega^2 \omega_{cz}^2]} \right|, \quad (36)$$

with $\omega_{cz} = eB_z/m_e$. This leads to a second order equation for the modulus of ω_{cz} ,

$$-\omega^2 S |\omega_{cz}|^2 \pm \omega_p^2 \omega |\omega_{cz}| + S(\omega_0^2 - \omega^2)[(\omega_0^2 - \omega^2) + \omega_p^2] = 0, \quad (37)$$

where S the sign of $[(\omega_0^2 - \omega^2)^2 - \omega^2 \omega_{cz}^2]$. The formal solutions are

$$\omega_{1cz} = \frac{-\omega_p^2 - (\omega_0^2 - \omega^2)}{\omega}, \quad (38)$$

$$\omega_{2cz} = \frac{(\omega_0^2 - \omega^2)}{\omega}, \quad (39)$$

$$\omega_{3cz} = \frac{\omega_p^2 + (\omega_0^2 - \omega^2)}{\omega}, \quad (40)$$

$$\omega_{4cz} = \frac{-(\omega_0^2 - \omega^2)}{\omega}. \quad (41)$$

The parameter region in which filtering occurs (k_- purely imaginary and $k_+ > 0$), is represented in Fig. 4 with a light shaded area (in the darker area both solutions are evanescent so there is total reflection). It can be divided into four ω subregions I, II, III, IV, delimited by the curve crossing frequencies $\omega = \omega_0$, $\omega = \omega_S \equiv (\omega_0^2 + \omega_p^2/2)^{1/2}$, and $\omega = \omega_{0p} \equiv (\omega_0^2 + \omega_p^2)^{1/2}$. The lower and upper bounds for the leftmost region I are the curves ω_{2cz} and ω_{3cz} [i.e., Eqs. (39) and (40)]; for region II, the curves ω_{4cz} and ω_{3cz} ; for region III, ω_{3cz} and ω_{4cz} ; and finally the bounds for region IV are the curves ω_{1cz} and ω_{4cz} . $\omega = \omega_S$ also marks a polarization mode change. In the light shaded areas, $(E_y/E_x)_{\pm} = \pm i$ if $\omega < \omega_S$, whereas $(E_y/E_x)_{\pm} = \mp i$ otherwise.

An additional constraint is set by the maximum available intensity of the magnetic field. It establishes a flat upper bound for ω_{cz} , and restricts the frequency range where filtering may be accomplished. The smallest fields could be used at or near the frequencies ω_0 and $\omega_{0p} \equiv (\omega_0^2 + \omega_p^2)^{1/2}$ where the boundary curves in Eqs. (38)–(41) touch the zero field axis. In practice the second one, ω_{0p} , would be more useful since

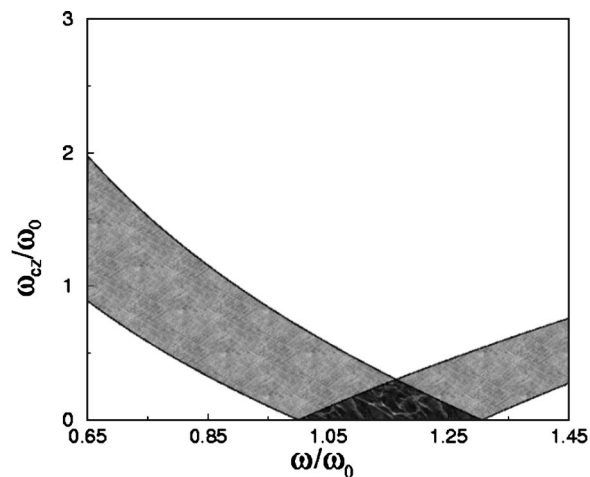


FIG. 4. Parameter region in which k_- is purely imaginary and $k_+ > 0$ (light shaded area) for $\omega_p/\omega_0 = 0.84$. The critical points where curve crossings occur are, from left to right, $\omega/\omega_0 = 1$ (it separates regions I and II), $\sqrt{1 + (\omega_p^2/2\omega_0^2)}$ (between regions II and III), and $\sqrt{1 + (\omega_p^2/\omega_0^2)}$ (between regions III and IV).

ω_p could be controlled in some cases, e.g., for a gas. Moreover, in general the possible perturbation on the filtering effect by absorption can be made negligible if the condition $(\omega^2 - \omega_0^2) \gg \omega \gamma$ is satisfied. In ω_{0p} this assumes the form

$$\frac{\omega_p^2}{\gamma \omega_{0p}} \gg 1, \quad (42)$$

where γ is the damping constant, see the Appendix. This ratio may be around 500 for realistic parameters in the near ultraviolet region [22], or near 20 for typical infrared absorption lines in ionic crystals [23]. Two other important factors that must be taken into account for the observability and potential application of the polarization filtering are the penetration length of the evanescent wave in the optically active medium, and the probability of the surviving mode.

The penetration length is proportional to the inverse of $\text{Im}(k_-)$. In practice the medium is not semi-infinite, of course, but the filtering effect may be achieved by a finite medium as long as it extends beyond the penetration length. In this case, using the transfer matrix technique, it can be seen that the polarization of the transmitted wave beyond the finite medium is equal to the one of the nonevanescent mode.

With respect to the probability of the surviving mode, the ratio $n_+ |C_+|^2$ between the energy flux of the surviving polarization and the incident energy flux is greater than 0.2 for $\omega_{cz}/\omega_0 > 0.2$ at $\omega = \omega_{0p}$ and $\omega_p/\omega_0 = 1$.

Finally, real materials hold multiple resonances and our theory has to be generalized by summing over them with appropriate oscillator-strength factors [20]. Thus, the previous analysis cannot be considered a full feasibility study for a practical implementation of the polarization selection, since a careful search of optimal materials and conditions is still required. The possibility to compete with other polarization methods will depend on the efficiency achieved, and other technical factors.

VI. DISCUSSION

In summary, we have shown that the atomic time-dependent Rabi oscillation and its suppression for moving atoms incident on a laser-illuminated region, is analogous to the time-dependent polarization rotation and its suppression for light pulses entering into an optically active medium. The eigenmodes in the laser region depend on Rabi frequency and detuning and in the optically active medium on the susceptibility matrix elements. Since ultrashort femtosecond pulses can be tracked experimentally by interferometric photon scanning tunneling microscopy (PSTM) [24], the time dependence of polarization rotation and its suppressions, by averaging, pulse splitting or filtering, can be tested experimentally. These effects may be of interest for the design of an all-optical quantum computer with information encoded, transferred or manipulated using the polarization state [25]; similarly, their atomic counterparts may be relevant in metrology and provide a mechanism for controlled quantum internal state preparation by projection or filtering, i.e., irrespective of the initial state, so that their experimental examination at a light-optics level is both feasible and worth pursuing. The optical analog of atomic state-filtering provides a way to produce polarized light. Whereas the atomic state may be selected by playing with the laser detuning and intensity, the polarization may be selected by a magnetic field.

We have emphasized the similarities between the atomic and the optical systems, but there are also differences worth noticing: the dispersion relations relating ω or E/\hbar with k are not equal and this leads to different evolutions of the light pulse or the atomic wave packet. Also, the two polarizations outside the active region are degenerate whereas, in general, the two orthogonal atomic internal components outside the laser region travel with different wave numbers.

ACKNOWLEDGMENTS

We are grateful to G. C. Hegerfeldt, D. Guéry-Odelin, A. Ruschhaupt, C. Salomon, and J. J. Gil for comments and encouragement, and to T. Pfau for his suggestion to examine an optical analog of Ref. [7]. This work has been supported by Ministerio de Ciencia y Tecnología (Grant No. BFM2003-01003-C03-03 and HA2002-0002) and UPV-EHU (Grant No. 00039.310-13507/2001 and 15968/2004).

APPENDIX A: SUSCEPTIBILITY TENSOR ELEMENTS

The general expressions for the elements of the χ tensor for a homogeneous dielectric in a magnetic field are obtained here from a simple, classical, Lorentz model. Each electron displacement from its equilibrium position \mathbf{r}_e is assumed to satisfy

$$m_e \frac{d^2 \mathbf{r}_e}{dt^2} = -e\mathbf{E} - e \frac{d\mathbf{r}_e}{dt} \times \mathbf{B} - K\mathbf{r}_e - m_e \gamma \frac{d\mathbf{r}_e}{dt}, \quad (\text{A1})$$

where K is an elastic force constant that keeps it bound, \mathbf{B} is a static, external magnetic field, m_e the mass of the electron, and γ a damping constant. (We neglect the small force due to the magnetic field of the optical wave.) Assuming that the applied electric field and \mathbf{r}_e vary harmonically as $e^{-i\omega t}$, and using for the macroscopic polarization $\mathbf{P} = -N e \mathbf{r}_e = \chi \epsilon_0 \mathbf{E}$, where N is the number of electrons per unit volume, and ϵ_0 the permittivity of the vacuum, a lengthy but straightforward calculation gives, for $\gamma=0$,

$$\chi_{11} = \omega_p^2 \frac{(\omega_0^2 - \omega^2)^2 - \omega^2 \omega_{cx}^2}{[(\omega_0^2 - \omega^2)^2 - \omega^2 \omega_c^2](\omega_0^2 - \omega^2)}, \quad (\text{A2})$$

$$\chi_{12} = \omega_p^2 \frac{\omega [i\omega_{cx}(\omega_0^2 - \omega^2) - \omega_{cx}\omega_{cy}\omega]}{[(\omega_0^2 - \omega^2)^2 - \omega^2 \omega_c^2](\omega_0^2 - \omega^2)},$$

$$\chi_{13} = \omega_p^2 \frac{\omega [-i\omega_{cy}(\omega_0^2 - \omega^2) - \omega_{cx}\omega_{cz}\omega]}{[(\omega_0^2 - \omega^2)^2 - \omega^2 \omega_c^2](\omega_0^2 - \omega^2)},$$

$$\chi_{22} = \omega_p^2 \frac{(\omega_0^2 - \omega^2)^2 - \omega^2 \omega_{cy}^2}{[(\omega_0^2 - \omega^2)^2 - \omega^2 \omega_c^2](\omega_0^2 - \omega^2)},$$

$$\chi_{23} = \omega_p^2 \frac{\omega [i\omega_{cx}(\omega_0^2 - \omega^2) - \omega_{cy}\omega_{cz}\omega]}{[(\omega_0^2 - \omega^2)^2 - \omega^2 \omega_c^2](\omega_0^2 - \omega^2)},$$

$$\chi_{33} = \omega_p^2 \frac{(\omega_0^2 - \omega^2)^2 - \omega^2 \omega_{cz}^2}{[(\omega_0^2 - \omega^2)^2 - \omega^2 \omega_c^2](\omega_0^2 - \omega^2)},$$

where

$$\omega_0 = \sqrt{K/m_e}, \quad (\text{A3})$$

$$\omega_c = eB/m_e, \quad \omega_{cu} = eB_u/m_e,$$

$$u = x, y, z, \quad (\text{A4})$$

$$\omega_p = \left(\frac{Ne^2}{m_e \epsilon_0} \right)^{1/2}, \quad (\text{A5})$$

are resonance, cyclotron, and ‘‘plasma’’ frequencies, respectively, and $B = (B_x^2 + B_y^2 + B_z^2)^{1/2}$.

In the Hermitian case, i.e., for $\gamma=0$, $\chi_{ij} = \chi_{ji}^*$. If $\gamma \neq 0$ the elements in Eq. (A2) would have the same form except for the substitution

$$(\omega_0^2 - \omega^2) \rightarrow (\omega_0^2 - \omega^2 - i\gamma\omega). \quad (\text{A6})$$

The other nondiagonal elements χ_{ij} can be obtained *formally* by taking first the complex conjugate of the expressions of the transpose elements χ_{ji} in Eq. (A2) and *then* making the substitution of Eq. (A6).

- [1] D. Mugnai and A. Ranfagni, in *Time in Quantum Mechanics*, edited by J. G. Muga, R. Sala, and I. L. Egusquiza (Springer, Berlin, 2002), Chap. 12.
- [2] A. Steinberg, in *Time in Quantum Mechanics*, edited by J. G. Muga, R. Sala, and I. L. Egusquiza (Springer, Berlin, 2002), Chap. 11.
- [3] N. F. Ramsey, *Molecular Beams* (Oxford University Press, New York, 1985).
- [4] S. Haroche, M. Brune, and J. M. Raimond, *J. Phys. II* **2**, 659 (1992).
- [5] J. Baudon, R. Mathevet, and J. Robert, *J. Phys. B* **32**, R173 (1999).
- [6] J. A. Damborenea, I. L. Egusquiza, G. C. Hegerfeldt, and J. G. Muga, *Phys. Rev. A* **66**, 052104 (2002).
- [7] B. Navarro, I. L. Egusquiza, J. G. Muga, and G. C. Hegerfeldt, *Phys. Rev. A* **67**, 063819 (2003).
- [8] Y. Sokolov, *Sov. Phys. JETP* **36**, 243 (1973).
- [9] V. Hannstein, G. C. Hegerfeldt, and J. G. Muga, *J. Phys. B* **38**, 409 (2005).
- [10] M. Büttiker, in *Time in Quantum Mechanics*, edited by J. G. Muga, R. Sala, and I. L. Egusquiza (Springer, Berlin, 2002), Chap. 9.
- [11] R. Sala, D. Alonso, and I. L. Egusquiza, in *Time in Quantum Mechanics* [Ref. 10], Chap. 8.
- [12] C. Bracher, *J. Phys. B* **30**, 2717 (1997).
- [13] R. Arun and G. S. Agarwal, *Phys. Rev. A* **64**, 065802 (2001).
- [14] V. Buzek, R. Derka, and S. Massar, *Phys. Rev. Lett.* **82**, 2207 (1999).
- [15] V. Gasparian, M. Ortuño, J. Ruiz, and E. Cuevas, *Phys. Rev. Lett.* **75**, 2312 (1995).
- [16] Y. Japha and G. Kurizki, *Phys. Rev. A* **60**, 1811 (1999).
- [17] M. Deutsch and J. E. Golub, *Phys. Rev. A* **53**, 434 (1996).
- [18] J. Y. Lee, H. W. Lee, and J. W. Hahn, *J. Opt. Soc. Am. B* **17**, 401 (2000).
- [19] V. S. Zaspaskii and G. G. Kozlov, *Opt. Spectrosc.* **78**, 88 (1995).
- [20] G. R. Fowles, *Introduction to Modern Optics* (Dover, New York, 1975).
- [21] L. Mandel and E. Wolf, *Optical Coherence and Quantum Optics* (Cambridge, New York, 1995).
- [22] K. E. Oughstun and G. C. Sherman, *Electromagnetic Pulse Propagation in Causal Dielectrics* (Springer, New York, 1994).
- [23] M. Fox, *Optical Properties of Solids* (Oxford University Press, Oxford, 2002).
- [24] H. Gersen, J. P. Korterik, N. F. van Hulst, and L. Kuipers, *Phys. Rev. E* **68**, 026604 (2003).
- [25] J. L. O'Brien, G. J. Pryde, A. G. White, T. C. Ralph, and D. Branning, *Nature (London)* **426**, 264 (2003).